Cortical Pathways During Postural Control: New Insights From Functional EEG Source Connectivity

Fabio Barollo, Mahmoud Hassan, Hannes Petersen, Isotta Rigoni, Ceon Ramon, *Life Senior Member, IEEE*, Paolo Gargiulo, and Antonio Fratini

***Abstract*— Postural control is a complex feedback system that relies on vast array of sensory inputs in order to maintain a stable upright stance. The brain cortex plays a crucial role in the processing of this information and in the elaboration of a successful adaptive strategy to external stimulation preventing loss of balance and falls. In the present work, the participants postural control system was challenged by disrupting the upright stance via a mechanical skeletal muscle vibration applied to the calves. The EEG source connectivity method was used to investigate the cortical response to the external stimulation and highlight the brain network primarily involved in high-level coordination of the postural control system. The cortical network reconfiguration was assessed during two experimental conditions of eyes open and eyes closed and the network flexibility (i.e. its dynamic reconfiguration over time) was correlated with the sample entropy of the stabilogram sway. The results highlight two different cortical strategies in the alpha band: the predominance of frontal lobe connections during open eyes and the strengthening of temporal-parietal network connections in the absence of visual cues. Furthermore, a high correlation emerges between the flexibility in the regions surrounding the right temporo-parietal junction and the sample entropy of the CoP sway, suggesting their centrality in the postural control system. These results open the possibility to employ network-based flexibility metrics as markers of a healthy postural control system, with implications in the diagnosis and treatment of postural impairing diseases.**

***Index Terms*— Brain network connectivity, EEG, postural control.**

Manuscript received January 26, 2021; revised May 2, 2021, October 5, 2021, and November 24, 2021; accepted December 28, 2021. Date of publication January 6, 2022; date of current version January 28, 2022. This work was supported in part by the School of Life and Health Sciences at Aston University, in part by the Institute for Biomedical and Neural Engineering at Reykjavík University, and in part by the Rannís Icelandic Research Fund (IRF) under Grant 174236-051. *(Corresponding author: Antonio Fratini.)*

This work involved human subjects or animals in its research. Approval of all ethical and experimental procedures and protocols was granted by Aston University's Research Ethics Committee under Application No. 1432.

Fabio Barollo is with the School of Science and Engineering, Reykjavik University, 101 Reykjavik, Iceland, and also with the Department of Biomedical Engineering, Aston University, Birmingham B4 7ET, U.K.

Mahmoud Hassan is with the School of Science and Engineering, MINDig, 35000 Rennes, France, and also with the School of Science and Engineering, Reykjavik University, 101 Reykjavik, Iceland.

Hannes Petersen is with the Department of Anatomy, University of Iceland, 101 Reykjavík, Iceland, and also with the Akureyri Hospital, 600 Akureyri, Iceland.

Isotta Rigoni is with the Department of Biomedical Engineering, Aston University, Birmingham B4 7ET, U.K., and also with the Neuroscience Department, Faculty of Medicine, University Hospital of Geneva, 1205 Geneva, Switzerland.

Ceon Ramon is with the Department of Electrical and Computer Engineering, University of Washington, Seattle, WA 98195 USA.

Paolo Gargiulo is with the School of Science and Engineering, Reykjavík University, 101 Reykjavík, Iceland.

Antonio Fratini is with the Department of Biomedical Engineering, Aston University, Birmingham B4 7ET, U.K. (e-mail: a.fratini@aston.ac.uk).

Digital Object Identifier 10.1109/TNSRE.2022.3140888

I. Introduction

EMERGING evidence has shown that the human brain is a network whose functions depend on the complex and dynamic interaction of highly specialized and spatially segregated regions [1]. Network neuroscience is a fairly new research field that employs graph theory techniques to assess brain functionalities and quantify the reconfiguration of neural pathways in response to tasks, stimuli, drugs administration, and treatments. The overwhelming complexity of the brain, which consists (on the micro-scale) of about 10^{12} neurons connected through 10^{15} synapsis [2], is abstracted (at the macro-scale) into a graph where nodes represent brain regions and edges represent their interconnections. In doing so, network neuroscience provides a powerful set of tools to quantify and investigate the intricate interactions that govern every brain function. Indeed, the insights it provides into the dynamic reconfiguration of connections between cortical regions is fundamental in understanding the deeply integrative functions of the brain, overcoming the limited view of a 'functional localization', where each segregated region attends to a specific function. Postural control is a primary example of a complex system, in which the Central Nervous System (CNS) coordinates and elaborates a vast array of signals, from visual cues to spatial orientation information from the vestibular system, to proprioceptive and somatosensory feedback from muscles and sensory organs [3]. Furthermore, the body of literature has shown how postural control is deeply related to structural and functional characteristics of the brain [4]. The relationship between postural control and cognitive functions has been extensively documented, highlighting in particular the effect of aging on brain plasticity and the consequent change in high-level strategies of postural control [5], [6]. The complexity of the cortical interactions that govern this process makes network neuroscience methodologies valuable tools,

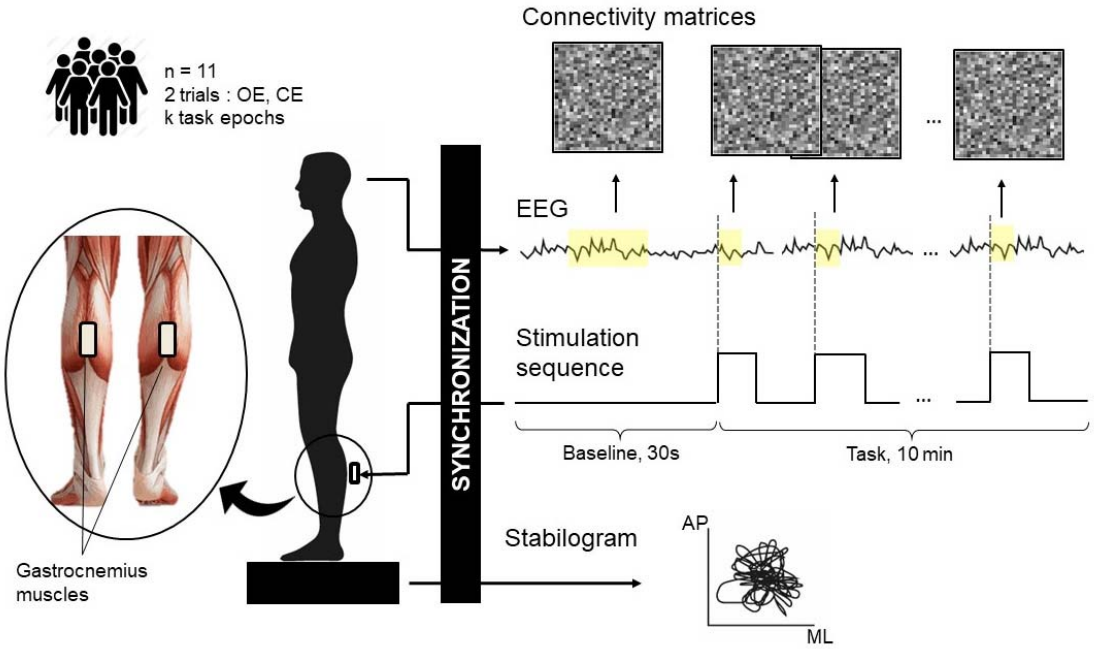

Fig. 1. Experimental set-up. Schematic representation of the experimental set-up. 11 volunteers made up the analyzed cohort, the single experimental session comprised two trials: eyes open (OE) and eyes closed (CE). The participant was asked to stand on a force platform in a quiet, upright stance. After 30 s of resting state (Baseline), a proprioceptive vibratory stimulation sequence was delivered through vibrators applied to the gastrocnemius muscles of the calves. The duration of the pseudo-random binary sequence was 10 min (Task), comprising k vibratory stimulation of variable length uniformly distributed between 1 - 6 s. The acquired EEG data, as well as the stabilogram signal (Anterior-Posterior and Medial-Lateral), were synchronized with triggers at the onset of each vibration. These triggers allowed for the definition of 1 second epochs (highlighted in the figure) from which, after the source reconstruction, network connectivity matrices were extracted.

although yet relatively unexplored, to investigate the role of the brain in postural control. Functional connectivity has been previously employed in literature to infer the organization of the cortex and most of the previous studies based their analysis on MRI data or scalp-level EEG [7]. In this work, on the other hand, we reconstruct brain networks combining non-invasive scalp EEG data with source reconstruction techniques. The approach adopted in the present study allows to evaluate brain networks based on the reconstructed cortical sources, exploiting the high time-resolution of the electroencephalographic signal while overcoming the well-established limitations of scalp-level networks. The purpose of this investigation is to show how scalp-EEG can be used to reconstruct the cortical network mechanisms that come into play during a postural control task in which the participant's quiet stance is disrupted by mechanical skeletal muscle vibrations. The effects of mechanical vibrations on muscle spindles are well documented in postural control literature [8], [9] and previous studies have employed them to provoke kinematic imbalances in order to assess the subjects postural responses [10]–[12], [13]. The analysis presented in this work includes the evaluation of static properties of the brain network as well as an assessment of its dynamic reconfiguration. Most importantly, this work highlights the relationship between network dynamics and stabilogram characteristics by correlating the dynamic flexibility of the network with the complexity of postural fluctuations. Previous studies showed how variations in the sample entropy of the sway signal, used as a complexity metric, were associated to varying levels of proficiency in the execution of postural task [14]. It is also well assessed how cortical plasticity (reflected in the flexibility of the brain network) is related to an enhanced ability of reaction to external stimuli [15]. In this work, we want to investigate whether a correlation between these two metrics exist and which cortical areas are involved. This study therefore set out to assess the potential for network-based analysis to be beneficial in the development of neurofeedback strategies, targeted at specific nodes (brain regions) of the cortical network and aimed at improving postural performance in subjects with age- or disease-related impairments.

II. Materials and Methods

Data were collected at Aston University's ALIVE research facility, following approval by the University Research Ethics Committee (ref: #1432). The recruitment of healthy adult volunteers (>18 years old) took place among the campus population. Exclusion criteria included the presence of any neuromuscular or balance disorders, physical limitations preventing a natural upright stance, ongoing medications and consumption of alcohol during the 24 hours prior to the experiment. 11 participants volunteered to take part in the study (age = 24.4±5.8, 5 males and 6 females, all indicating their right leg as the dominant one). The experiment was carried out in one single seating of about 1.5h, including the participant's preparation. A schematic of the experimental set-up is depicted in Figure 1. Participants were asked to stand still on a force platform, maintaining a natural upright posture and fixing their gaze on a marker on the wall in front of them, at about 2m distance. After 30 s of baseline recording, a randomized sequence of mechanical vibratory stimuli was

applied to the participants gastrocnemius muscles of both legs in order to disrupt their stance. The stimulation sequence had a duration of 10 min and consisted of a randomized pulse wave in which both pulse width and inter-stimulus intervals were uniformly distributed between 1 and 6 seconds. The vibration was delivered at 85 Hz, via two small eccentric rotating mass DC motors (ERM) encased in a plastic cylinder and attached to the participants' calves (diameter: 30mm, length: 62mm). This set-up was based on previous works reported in [10], [16]. The session (30 s baseline followed by 10 min stimulation) was repeated twice, with eyes open (OE) and closed (CE), in randomized order. The EEG signals were recorded using a 64-channel wet electrodes cap with a standard 10-20 system montage (AntNeuro, Enschede - Netherlands). The recording sampling frequency was $f_S = 1000$Hz. Participants were instructed to keep their facial muscles as relaxed as possible, avoiding teeth grinding and jaw clenching, in order to minimize muscle artifacts in the recorded signal.

Participants stood on an AMTI OR-6-7 force platform (part of a motion capture system by Vicon Motion Systems Ltd, Kidlington - UK) that measured their center of pressure trajectory (CoP) over the course of the experiment, in its anterior-posterior (AP) and medial-lateral (ML) components, at a sampling frequency of $f_S = 1000$Hz. A customized wearable electronic box was developed and built in order to generate the randomized pulse wave that regulated the calf stimulation and to simultaneously send a series of 5V TTL trigger signals to the EEG amplifier and to the force platform system. The 5V trigger signals were generated at the onset and offset of every vibration and allowed for the synchronization of EEG and CoP data, as well as their segmentation into epochs. The 3D printed box case was secured on a belt so that the participants could wear it around their waist. The device was powered with two rechargeable 9V batteries, while an internal voltage regulator made sure to deliver the appropriate voltage (12.4V) for the two connected ERM motors to deliver a 85 Hz vibration (corresponding to a rotational speed of the internal eccentric mass of 5100 RPM).

III. Data Analysis

A. Preprocessing

The steps followed for the preprocessing of the EEG signal were adapted from a semi-automated pipeline presented in the software Cartool [17] and implemented with custom-made Matlab scripts. The EEG signal was filtered between 1 - 45 Hz with a zero-phase band-pass FIR filter; the DC offset was subsequently removed from the whole signal before segmenting it into epochs. Epochs were defined as 1 second long signal segments after each onset trigger, corresponding to the 1 second of electric brain signal after the start of each vibration of the sequence. The epoch length of 1 second was chosen in that it is the maximum length that allows to avoid overlapping with the following vibration/rest cycle of the sequence.

Three frontal electrodes (Fp1, FpZ, Fp2) were used to perform an Electrooculography (EOG) regression on the remaining 60-channel data, in order to remove eye blink artifacts [18]. Channels with poor signal quality were identified within every segmented epoch and replaced with an interpolation of the neighboring channels signals. The classification of 'bad channels' was performed with a supervised automated approach, based on the standard deviation (std) of the signal. The i^{th} channel was classified as 'bad' if its std_i exceeded the average std (computed among all the channels) times a certain constant threshold value T.

$$if\ std\ i > T * std \Rightarrow Interpolate\ channel\ i$$

The outcome of this preprocessing step was visually inspected to evaluate the effectiveness of different T values. The value $T = 1.7$ was finally chosen, as it proved to be consistent with the choices that would have been made with a purely visually inspected manual rejection. The interpolated channels were filtered between 1-45 Hz again to smooth them out. Epochs where more than 15% of the total channels were interpolated ($\geq$9 channels) were discarded. Finally, the EEG signal was re-referenced to the common average. Table I, in the Appendix section, provides an overview of the total number of vibratory stimulations applied to each participant, and the final amount of accepted epochs following the preprocessing of the data. The AP and ML components of the CoP trajectory were detrended and filtered between 0.2 - 20Hz with a bi-directional bandpass Butterworth filter [19]. The signal was then normalized to unit variance by dividing it for its standard deviation [20].

B. Reconstruction of Functional Brain Networks

Functional brain dynamics were reconstructed using the '*EEG source connectivity*' method [21], [22]. This method was proposed with the aim to overcome the volume conduction and field spread limitations that affect scalp-level networks by performing functional connectivity network analysis at the cortical level. First, this approach requires to reconstruct the cortical sources by solving the inverse problem [23]. Given an equivalent current dipole model, the scalp EEG signal recorded on M channels can be expressed as the linear combination of P time-varying current dipole sources [24]:

$$X(t) = G * S(t) + N(t)$$

where G is the lead-field matrix of size *[M, P]*, that weighs the contribution of each source towards the recorded signal, S(t) is the matrix containing the sources time series *[P, Timepoints]* and N(t) is the noise covariance matrix. Solving the inverse problem consists in finding an estimate $\hat{S}(t)$ of the source matrix. For this study, a three-layer BME model (brain, skull, scalp) was adopted to define the inverse problem domain. The model's morphology was based on a standard head model template provided by BrainStorm [25]. To solve the inverse problem, we used the weighted Minimum Norm Estimate (wMNE) algorithm [26], [27]. The output consists of 1500 estimated source time series, localized at the cortical boundary. For the purposes of network analysis, the brain is rendered through a graph in which nodes represent cortical regions. In the present work the Desikan-Kiliany anatomical atlas was employed to parse the cortex into 68 regions

of interest (ROIs) [28]. By averaging the estimated source time series within each regional boundary, the regional time series matrix is obtained (with dimension *[68, Timepoints]*). Functional connectivity (FC) was computed based on the Phase Locking Value (PLV), a measure of statistical coupling between the cortex-level regional time series. The advantages and limitations of different connectivity metrics have been extensively reviewed in literature [29] and previous research on simulated data showed that the combination of wMNE and PLV has the highest accuracy in terms of similarity with the reference network [30].

Functional connectivity values between each pair of the 68 brain regions were computed for every 1-second epoch in three frequency bands: Alpha ($\boldsymbol{\alpha}$, [8-13] Hz); Beta ($\boldsymbol{\beta}$, [13-30] Hz); and Gamma ($\boldsymbol{\gamma}$, [30-45] Hz).

C. Nodewise and Edgewise Static Analysis

The focus of static network analysis is to investigate the global characteristics of the brain network during the execution of the postural control task, without taking into account its dynamic evolution. Therefore, connectivity matrices within each trial (OE and CE) were averaged to obtain a single task-related connectivity matrix for every subject and frequency band. This averaged matrix was then thresholded in order to keep only the top 10% strongest connections, while removing weaker, spurious connections [30], [31]. Many network measures are available to characterize different aspects of the brain connectivity, providing insights on local and global properties of the network structure. First, we analyzed local parameters of single nodes of the network, i.e. cortical regions, to characterize their properties and map how their role in the network changes in different experimental conditions (nodewise analysis). Then, we used Network-Based Statistics (NBS), to give a global representation of the network reconfiguration in the two conditions, by focusing on the inter-region connections themselves (edgewise analysis) [32]. The degree of a node is one of the easiest and most common local network measures; it consists in the number of connections (edges) associated to that specific node. A generalization of this measure is a node's strength, which comes into play when weighted networks are considered and consists in the sum of the weights of the edges related to the node. Degree and Strength are considered measures of hubness, as they describe how central a node is in the network by providing information on the number of connections it is involved in and their weight. These measures help to determine whether the node is a highly interconnected one (hub) or if it is a marginal, isolated node in the network. The strength parameter was computed for each of the 68 brain regions, in $\boldsymbol{\alpha}$, $\boldsymbol{\beta}$ and $\boldsymbol{\gamma}$ frequency bands and a statistical analysis was carried out to investigate the presence of a significant difference between the two experimental conditions of open eyes and closed eyes. The non-parametric Wilkoxon signed rank test was chosen given the limited sample size (11 repetitions) and the lack of assumption on the normal distribution of the data. The resulting p-values were subsequently corrected for multiple comparisons using the False Discovery Rate (FDR) method. The same analysis was performed on the baseline connectivity matrices obtained from the initial 30 s resting-state epochs, during both conditions (OE and CE). This allowed to verify the presence of differences in nodes strength solely related to the visual input (or lack of thereof), in the absence of vibratory simulation. Then, for an edgewise analysis of the network, differences in the connectome were investigated using the NBS method. The method was implemented in Matlab using the NBS toolbox [32]. NBS works on the connectivity matrices representing the network in the two testing conditions, organized according to a statistical model specified in terms of the general linear model (GLM). It provides as an output the set of connections comprising the network that is found to show a significant difference in the two conditions, with an associated p-value. The significance level was set at 0.05 (with correction for multiple comparisons using permutation test) and the number of iterations at 5000. The network analysis was performed both on task (during the stimulation) and baseline connectivity matrices.

D. Dynamic Analysis–Flexibility/Complexity Correlation

The network dynamic was assessed by computing the flexibility index of each node over the execution of the postural control task. First, the connectivity matrix that identifies the functional network is computed for every 1s epoch following each onset of the binary vibratory sequence throughout the duration of the experiment. Every network of this sequence is decomposed into its dynamic modules, using the community Louvain algorithm [33]. Modules represent sets of highly intra-connected regions that are weakly connected with others [34]. The flexibility of each node of the network is then computed based on the number of times the affiliation of the node shifts among different modules. Subsequently, a posturographic analysis was performed on the force platform data to extract the sample entropy (S_{EN}) from the anterior-posterior (AP) and medial-lateral (ML) components of the center of pressure (CoP) trajectory. This allowed us to quantify the complexity of the postural signal for each participant during the execution of the task. Finally, Pearson's linear correlation coefficient was computed in both experimental conditions (OE and CE) between the flexibility values of each of the 68 nodes and both the S_{EN} values of the AP and ML sway respectively (number of repetitions corresponding to the number of participants). A p-value was also provided together with the Pearson's coefficient by running a Student's t-test for each comparison, testing the null hypothesis of no correlation.

IV. Results

This chapter illustrates the outcome of the functional connectivity analysis. The results of the static analysis are reported in sections *A* and *B*, which summarize, respectively, the nodewise and edgewise comparisons of the global brain networks during OE and CE tasks. Paragraph C, instead, focuses on the dynamic analysis and reports the results of the correlation analysis performed between the flexibility index of each node and the complexity of the CoP sway. The following results

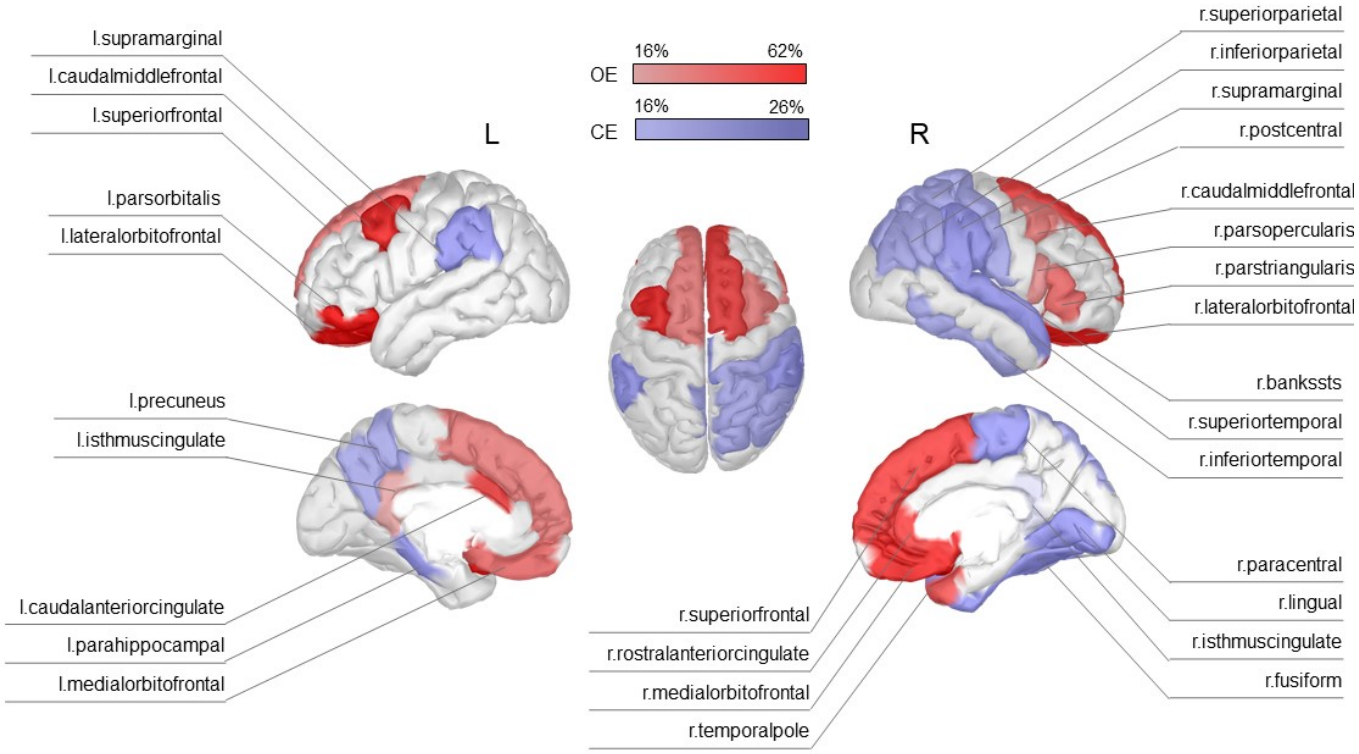

Fig. 2. Nodewise static analysis results. Percentage variation in each region's strength during the postural task in the two conditions of open (OE) and closed eyes (CE), in the alpha band. The anatomical representation displays the nodes of the network as the corresponding 68 cortical regions, parcellated according to the Desikan-Killiany atlas. The brain is shown from the top as well as in the medial and lateral view of each hemisphere. Regions highlighted in red displayed higher strength values during OE, regions highlighted in blue showed higher strength values in CE. The saturation of the color denotes the amount of percentage increase, as shown by the color bar. Only regions with a statistically significant difference in strength are reported (FDR-corrected p-value smaller than 0.05).

refer to the analysis in alpha, as statistically significant results only emerged in this frequency band.

A. Static Analysis – Nodewise

Significant differences in nodes strength values between OE and CE tasks emerged from the nodewise static analysis. The outcome of the strength analysis is displayed in Figure 2. The results highlight two main contiguous areas with a different characterization, the frontal regions with higher strength values during OE and the right parieto-temporal regions where higher strength values can be observed during CE.

An increased strength can be observed during the OE task in the network nodes corresponding to the frontal areas of the cortex (Orbitofrontal: left medial, $p = 0.033$; left lateral, $p = 0.036$; right medial, $p = 0.015$; right lateral, $p = 0.015$. Superior-frontal: left, $p = 0.036$; right, $p = 0.015$) as well as the anterior cingulate (left caudal, $p = 0.033$; right rostral, $p = 0.015$). These results present a distinct symmetry between the two hemispheres and a marked percentage increase in strength ($>50\%$ increase over the CE task) can be noted especially in the orbitofrontal regions (left lateral, $p = 0.036$; left medial, $p = 0.033$; right lateral, $p = 0.015$; right medial, $p = 0.015$) as well as in the left pars-orbitalis ($p = 0.024$).

On the other hand, network nodes whose strength increased during the CE task, are not symmetrically distributed across the hemisphere but involve predominantly the right one. The corresponding cortical regions in the right hemisphere are focused in the central (post-, $p = 0.031$; para-, $p = 0.036$), parietal (superior, $p = 0.015$; inferior, $p = 0.033$) and temporal (superior, $p = 0.036$; inferior, $p = 0.015$) areas. An increase in the supramarginal region can also be observed in both hemispheres (left, $p = 0.033$; right, $p = 0.033$). Overall, it must be noticed that the percentage increase in strength during CE in these regions is not as pronounced, the maximum value is a 25% increase over the OE task. The baseline analysis, in which strength values extracted from the connectivity matrices related to the quiet stance epochs, in OE and CE conditions, were tested, didn't provide any significant differences. The lack of significant variation in node strength values between OE and CE during the baseline epochs suggest that the significant results emerged from the task analysis in the two experimental conditions are actually related to the proprioceptive vibratory stimulation. Table II, in the appendix section, provides a complete overview of the results for each cortical region, including the mean strength values computed over the participants, their standard deviation, the strength percentage increase values and the associated corrected p-values.

B. Static Analysis –Edgewise

The results of the edgewise static analysis are depicted in Figure 4 in the appendix section. The network reconfiguration

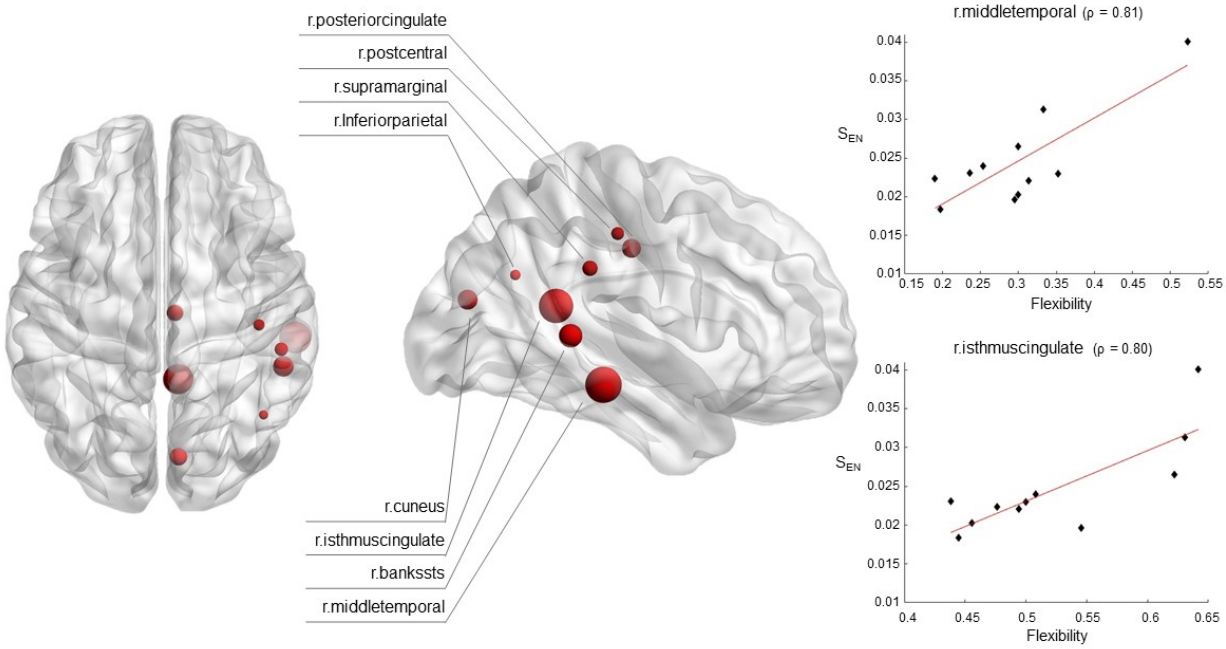

Fig. 3. Results of the correlation analysis between network flexibility during OE task and sample entropy of the AP component of the postural sway. The highlighted regions correspond to the nodes of the network whose flexibility correlated with the corresponding S_{EN} of the posturographic signal in a statistically significant way ($p < 0.05$). Each of these regions is represented with a node whose size is proportional to the associated Pearson's correlation coefficient (ρ). The figure also shows the correlation scatter plots (including regression lines) related to the two regions with highest Pearson coefficients; flexibility values are in the x-axis while the sample entropy index is in the y-axis.

in the alpha band between OE and CE tasks, as evaluated by the change in connectivity values, involves 116 edges of the network, all of which showed increased connectivity during the CE task. The resulting network is spatially localized in the posterior areas of the brain, presenting connections across the hemispheres, as well as intra-hemisphere connections on the right side. The significant connections are predominantly temporo-parieto-central, involving mainly the parietal (superior and inferior), the central (post and para) and the temporal (inferior and middle) brain regions. These results, in terms of cortical regions involved and predominance of the right hemisphere, are in accordance with the nodewise analysis results reported for the CE task in the previous section. The analysis on the baseline network reconfiguration in the two experimental conditions highlighted 160 significant edges, whose connectivity values increased during CE. The resulting network partly overlaps with the task-related one, especially in the parietal and temporal regions; at the same time, though, it also differentiates itself with regards to its edges distribution. Specifically, it doesn't present a strong right lateralization of intra-hemispheric connections while it displays a higher connection density in the frontal lobe, which was previously unobserved. Nevertheless, the statistical test (NBS) didn't highlight any statistically significant difference between the task-related and baseline-related networks. A complete list of the cortical regions involved in both networks, with the corresponding degree value, is available in Table III of the appendix section.

C. Dynamic Analysis – Flexibility/Complexity Correlation

In the dynamic analysis we tested the correlation, in the alpha frequency band, between node flexibility and S_{EN} values of the CoP sway (in the OE and CE experimental conditions and in the AP and ML sway components). Significant Pearson's correlation ρ values emerged between the flexibility of nodes in OE condition and the corresponding AP stabilogram sway.

In this case, significant correlation values were found in the postcentral, supramarginal and inferior parietal areas as well as in the temporal-occipital regions and the cingulate cortex of the right hemisphere (see figure 3). Specifically, high Pearson coefficients ($\rho > 0.70$) could be observed in areas of the cingulate cortex (isthmus cingulate $\rho = 0.80$, $p = 0.003$ and posterior cingulate $\rho = 0.69$, $p = 0.019$) as well as in the temporal-occipital cortex (middle temporal gyrus $\rho = 0.81$ $p = 0.002$ and cuneus $\rho = 0.7$ $p = 0.018$).

Table IV of the appendix section reports the Pearson coefficient and corresponding p-value for each significant region. Average S_{EN} values of the AP and ML sway, together with their SD, are provided for baseline and task, in OE and CE, in Table V of the appendix. The table also reports the p-values resulting from the Wilcoxon signed-rank tests performed within and between conditions (baseline vs. task, and OE vs. CE respectively).

V. Discussion

Postural control is the phrase used to indicate the complex regulatory system whose aim is to maintain a stable upright stance. The complexity of this task lies in its reliance from a wide range of sensory inputs gathered predominantly through the visual, somatosensory, proprioceptive and vestibular systems. While early research on the topic associated postural control with a reflex response enacted at the level of the brainstem and spinal cord [35], extensive recent evidence pointed

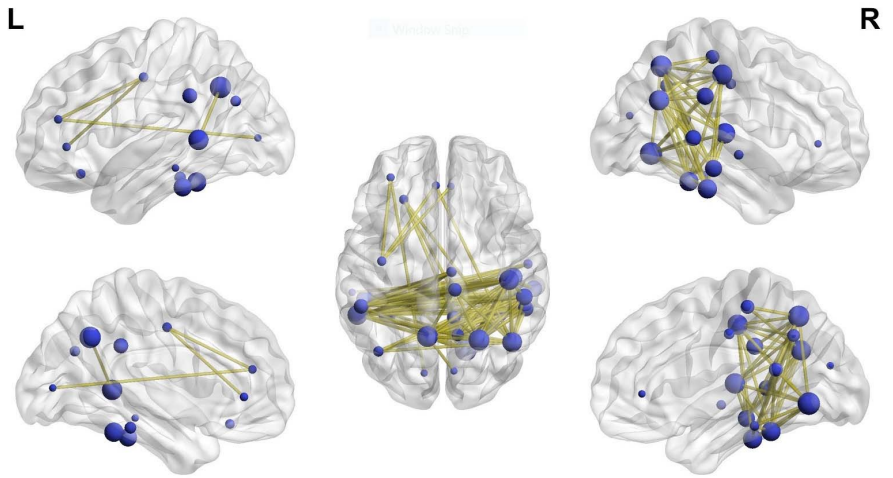

(A) Task

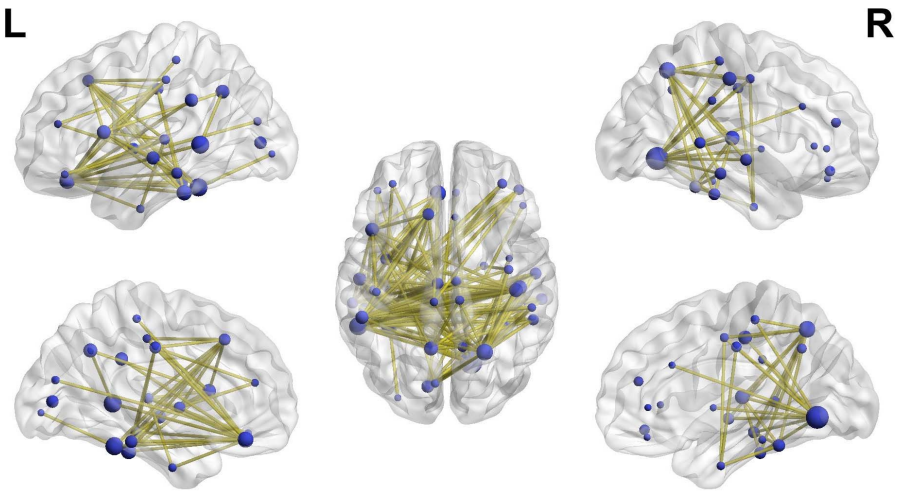

(B) Baseline

Fig. 4. Edgewise static analysis results. Graphical representation of the network reconfiguration occurring in the alpha frequency band. Cortical regions are represented as nodes of the network, while edges represent the connections between the regions. The size of each node is proportional to its degree, i.e. the number of connections in which it takes part. The figure highlights the differences between the brain network structures in the two experimental conditions (OE and CE), after the respective connectivity matrices were compared and tested to identify edges which underwent a significant change in connectivity value. Figure A depicts the 116 edges that showed a statistically significant difference in connectivity (significance level of NBS set to 0.05) during the task execution, i.e. average of 1s epochs following the onset of each vibratory stimulation. All of them are associated with higher connectivity values during the CE task. In the same way, Figure B shows the 180 edges associated with significantly different level of connectivity during the baseline epoch, i.e. no vibratory stimulation. In this case too, all of the edges are associated with higher connectivity values in the CE condition.

out the crucial role of the cortex as a hub for the processing of sensory information and the subsequent development of an effective postural control strategy [36].

Balance perturbations techniques have been extensively used to challenge the upright stance in order to investigate the elicited postural response. In the present work the disruption of the participants quiet upright stance was induced by skeletal muscle vibration of the lower limbs, in which a randomized binary vibratory sequence was applied to the gastrocnemius muscles of the calves.

The characteristics of the cortical network structure in the two experimental conditions of open and closed eyes, as well as the dynamic reconfiguration of the network in relationship with the posturographic data, were investigated using 68 regional time-series obtained from reconstructed cortical sources, averaged according to an anatomical atlas as presented in the methodology section of this work. To our knowledge, the use of EEG source connectivity to characterize functional networks involved in postural control has been scarcely used in previous works, since most of the previous studies on the topic relied on scalp-level EEG data [37]. The scalp-level approach, though, presents limitations (most notably distortions introduced by the volume conduction effect) that have been extensively highlighted and discussed in literature [38]. The results which emerged from this investigation, consistently highlighted the presence of statistically significant cortical network structures in the alpha band ($\boldsymbol{\alpha}$: [8-13] Hz). This is in line with results from previous literature which showed the role of alpha band connectivity in cortical processes related to postural control tasks [37], [39].

Cortical effects were also previously reported in beta band during balance tasks [39], [40]. It is worth noting, though, that the majority of previous literature focuses on cortical activation in terms of spectral and power-based analyses, while the novel methodology proposed in this work involves functional connectivity which relies on phase metrics (PLV) and therefore focuses on the cortical signals' phase synchrony rather than their amplitude.

A. Discussion of Nodewise OE Results

The results of the nodewise analysis, in which we compared the node strength in the two experimental conditions, display two clear and well-defined clusters of regions. The OE condition is marked by an increased node strength in the orbitofrontal, superior-frontal and anterior cingulate regions of the cortex, which characterizes them as central hubs of this brain network. Previous research has shown how the frontal lobe plays a role in the allocation of attentional resources during motor performances [41]. In particular, the caudal and middle-frontal regions comprise the Frontal Eye Field (FEF), which is related to visual field perception and awareness and the maintenance of attention to peripheral locations [42]. FEF is also part of the Dorsal attention Network, which has been shown to be a center of top-down control of visual attention [43]. Moreover, besides being involved in spatial attention, it has been suggested that offline motor planning is one of the core function of this network, i.e. the representation of abstract kinematic movement, which would indicate the evolution of this network from a role of pure motor control to a much wider range of cognitive functions [44]. This motor attention frontal area interplays with the orbitofrontal cortex (lateral- and medial-orbitofrontal regions) which is a heterogeneous region acting as a center for sensory integration [45] as well as with the anterior cingulate cortex (caudal- and rostral-anterior cingulate regions), which has been traditionally related to decision-making and has been shown to play a role in the recognition of unstable posture [46], [47]. These findings suggest that the reaction to a challenged upright stance, during the OE condition, engages an attention-related network in the alpha band located predominantly in the frontal lobe, with the visual information playing a predominant role in the integration of the postural control feedback system. They also highlight the reliance on visual cues in the detection of postural instability and the subsequent development of a corrective strategy. These results also accord with and corroborates the observations of previous studies which showed how certain cognitive functions, namely attention, interact with motor function and postural control [41], [48], [49].

B. Discussion of Nodewise and Edgewise CE Results

Observing the results of the nodewise analysis for the CE condition, on the other hand, it clearly emerges a predominance of the parietal and temporal lobes. Another noticeable feature of these results is the asymmetry of the network nodes involved, which are primarily localized in the right hemisphere. The increased hubness of these nodes in the network organization associated with a postural response in the absence of visual cues is also supported by a qualitative inspection of the task edgewise analysis, which however didn't provide statistically significant differences when compared the baseline network. The analysis conducted on the network connections in the two experimental conditions, highlights the strengthening of inter-hemisphere connections among parietal and temporal regions as well as a dense network of intra-hemisphere connections in the right side of the brain, during the CE condition. These results are backed by a strict network-based statistical analysis that confirms the significance of the displayed connections. The emerging network clearly highlights the involvement of the parietal lobe. The Anterior parietal cortex (APC) is the main recipient of proprioceptive signals. While commonly identified as a whole with the primary somatosensory cortex, APC actually comprises of four areas distinctively defined by their cytoarchitecture. It has been shown how two of these areas in particular (Brodmann's 3a and 2) are the primary target for proprioceptive information regarding muscle fibers lengthening, joints position, etc. [50]. The Posterior parietal cortex (PPC) is a hub of multisensory integration, being responsive to visual, auditory and vestibular solicitations which is also involved in motor planning functions. The superior and inferior parietal lobules are in fact centers of interpretation of sensory information involving body image and spatial perception. Previous studies reported how parietal lesions are linked to disturbances in motor behavior resulting from the failure to gather contralesional space information by limb movement [51]. The network connections between parietal cortex and temporal regions (in particular superior temporal) suggests an involvement of what has been identified as the vestibular cortex. In order to properly identify the nature of a perceived motion, distinguishing between motion of the surrounding environment from self-motion, and resolve discrepancies in the visual signal, the brain relies on the integration of vestibular signals from the inner ear's sensors. The broad range of interactions that the vestibular system has with other sensory systems is reflected in its distributed cortical network. The exact localization of this network has been amply investigated and discussed in literature, both in human and non-human primates [52]. The network that emerges from the edgewise results, with a significant strengthening of the superior-temporal region and of the areas surrounding the posterior end of the lateral sulcus (Sylvian fissure) reflects what is commonly defined as the parieto-insular vestibular cortex (PIVC). This area has been hypothesized to be involved in a vestibular cortical pathway that spreads from the temporal parietal junction (TPJ) to the retro-insular cortex (RI) and is active in the integration of visual and vestibular information for a self-referential processing that informs about self-location in space [52]. More recent literature further investigated the anatomical and functional characteristics of this area, identifying two main components to the vestibular cortex: PIVC and Posterior-insular cortex (PIC) [53]. Both areas are involved in the processing of vestibular cues, but they differ in the way they respond to visual stimulation. It has been shown that PIC processes visual clues related to self-motion while PIVC's activity is inhibited in the presence of visual signals, to avoid visual-vestibular conflict. Despite the limits of the adopted

brain parcellation that doesn't allow to discriminate between these two subregions, this functional dynamic suggests that, giving the lack of visual cues during the CE task, the presented results reflect the activation of PIVC.

Overall, these findings characterize a cortical network that operates in alpha band and manifests itself in the coordination of a reaction to a mechanical postural challenge in the absence of visual information. The network reconfiguration in the two experimental conditions, in the wake of the postural challenge, was evident in the characteristics of single nodes, namely in their different characterizations as central hubs of the network, as pointed out by the comparison with the baseline nodewise results. These results highlight how in order to counterbalance the disruption of the upright stance and prevent falling, the postural control system heavily relies on the elaboration of proprioceptive and vestibular information. The asymmetry of the network further suggests the significant involvement of the vestibular cortex, which is characterized by a right hemispheric dominance in right -handed people (the entirety of the analyzed cohort) [54]. Moreover, the highly demanding postural task characterized by the lack of visual cues and the consequent challenge presented by the necessity to rely solely on proprioceptive and vestibular information, might explain the predominance of strongly interconnected regions in the right-hemisphere, i.e. the contralateral somatosensory areas to the non-dominant leg (all the participants have in fact identified the right leg as their dominant one). This interpretation is in accord with previous research which linked postural fatigue and absence of visual information with enhanced reliance on somatosensory information from foot and ankle for the control of upright stance [55]. A qualitative inspection of the network resulting from the task edgewise analysis seems to confirm this interpretation, showing significant connections among the same network hubs emerging from the nodewise analysis in the parieto-temporal, vestibular cortex. Nevertheless, at the wider level of network structure, the brain reconfiguration in OE and CE, following the proprioceptive stimulation, was not statistically different from the resting state network before the stimulation. This is a limitation of the current work, which will benefit from a more in-depth further analysis, and is possibly due to the limited sample size, the design of the experimental paradigm or the necessity to identify more suitable network comparison metrics. Another aspect worth of consideration in following studies is the lack of significant differences in node strength in resting state between the two conditions, which suggests the need to explore other local network properties other than hubness (e.g. modularity, clustering, centrality, etc.). However, the baseline edgewise analysis, which provides a more global picture of the network topology reconfiguration, indeed showed significant changes in the two resting state conditions. This baseline analysis indicates that the observed differences are most likely related to the presence of visual cues (or lack of thereof). This observation, which requires further investigation, suggests the predominance in the network of those cortical pathways related to the processing of visual information which seem to 'overshadows' the effects on the network reconfiguration of vestibular and proprioceptive related strategies to counteract the postural disruption.

C. Flexibility - Complexity Correlation

The flexibility of a node is determined by how often its modular affiliation changes over the course of the experiment. Since modules are clusters of highly interconnected nodes often associated with specialized functions, the flexibility of a given node points at the ability of the corresponding brain region to be involved into multiple functions [56]. Prominently among other brain network properties, flexibility has been widely used in literature as a biomarker to capture neuroplasticity differences across individuals and its correlation with cognitive performance has been documented during memory and attention training as well as motor tasks [57]–[60].

Previous literature has also highlighted how healthy physiological processes such as postural control are characterized by a complex dynamic and complexity in the fluctuations of the CoP signal has been commonly used to investigate the effectiveness of the postural control system [61]–[63]. At the same time, it has been shown how age- or disease-related impairments, associated with worsening postural performance translate into a loss of complexity of the posturographic signal. Thus, if on the one hand, highly flexible networks are associated with greater brain plasticity and the ability to develop adaptive strategies to counteract external disruptive stimuli, on the other hand, more complex CoP fluctuations (characterized by higher S_{EN} values) reflect an enhanced automaticity of the postural control system [20]. The correlation between cognitive decline and balance, especially in relationship with the incidence of falls has been extensively discussed in literature [6], [36], [64]–[66]. This highlights the necessity of developing targeted therapies to mitigate fall risk as well as the opportunity for the design of neurofeedback strategies aimed at improving postural performances in ageing population or cognitively impaired subjects. In order to do this, it is first necessary to identify the specific cortical regions to target and markers that can be correlated with postural performance. Observing the results, it can be noticed that the regions that displayed a significant correlation with the complexity of the anterior-posterior CoP fluctuation encompass predominantly parts of the cingulate, parietal and temporal cortices. The results once again highlight the role of cortical centers of proprioceptive and vestibular processing, with the involvement of APC/PPC and the regions surrounding the lateral sulcus (PIVC). The inferior parietal cortex, whose role in spatial perception and body image neural representation has been previously discussed, appears involved as well. Of particular interest though, is the high correlation that emerged in the cingulate cortex and in the middle temporal and cuneus areas. The posterior cingulate cortex (PCC) has been associated with the main function of visuospatial orientation, and of integrating neural representation of self-location and body ownership acting as a mediator in the interplay between different cortical areas in the parietal and medial temporal regions [67]. Moreover, previous research has shown the PCC's centrality as a node

within the default mode network (DMN) and highlighted its high metabolic activity and dense structural connectivity with widespread brain regions which characterize it as a central cortical hub [68]. Furthermore, it has been suggested that PCC plays an active role in cognition, as indicated by its reduced metabolism in Alzheimer's disease and ageing patients. While the functions of this cortical regions are still being investigated, there is clear evidence of its involvement in cognition control through signaling of environmental changes [69]. It appears clear then, how the flexibility of such a deeply interconnected processing hub of the cortex is necessary in order to effectively react to environmental challenges, such as a motor perturbation of equilibrium represents. The results also offer an indication of the likely involvement of certain visual pathways, especially considering the correlation observed between the posturographic signal complexity and the flexibility of cuneus and middle temporal regions. Cuneus is a region of the occipital lobe which is most known for its involvement in basic visual processing and for its role as a mediator in the exchange of visual information between the primary visual cortex (V1) and extrastriate cortices such as the middle temporal visual area (MT/V5) [70]. The involvement of the middle temporal gyrus further points towards a possible role of the MT/V5, a functional area of the extrastriate visual cortex located at the boundary with the occipital lobe [71]. This area is part of the visual cortex and in particular it is involved in the dorsal visuospatial pathway, also referred to as 'motion' pathway [72]. MT is in fact a motion-sensitive cortical region involved in a range of functions including directing attention in the visual environment, integration of local motion signals and kinematic recognition. Its critical role in motion perception has been extensively documented, showing how lesion to MT/V5 adversely affects motion perception [73], [74]. Both cuneus and middle temporal regions play a complex role of mediators in visual processing pathways and project to a number of satellite cortical areas in charge of complementary cognitive functions especially related to motion detection. These characteristics might explain why a more flexible dynamic behavior in these regions, i.e. their ability to shift affiliation between different network modules, is reflected in an overall more successful postural strategy, as highlighted by the high correlation values with the S_{EN} of the CoP trajectory.

Nevertheless, a note of caution is due in this interpretation, especially concerning the role of the MT/V5 area, as it may be somewhat limited by the anatomical atlas used. In fact, recent tractography-based parcellation of the middle temporal gyrus identified four distinct subregions based on anatomical connectivity, each one being associated with unique functions in a wide range that includes sound recognition, semantic retrieval, language processing and decoding gaze direction [75]. The aspect of auditory influence on postural control, in particular, has been discussed in previous works and its effects at a cortical network level requires a more in depth investigation [76], [77]. Therefore, the 68-region cortical anatomical atlas employed in this study does not provide the required detail of parcellation that would allow us to positively identify, within the broader middle temporal gyrus region, the specific area involved as the MT/V5 and thus infer with certainty on its direct involvement in the postural control system. Furthermore, it is worth noting that significant flexibility/S_{EN} correlation emerged only during the OE task. This aspect requires further investigation and possibly an improved experimental protocol. Overall, future developments of this research will benefit from the involvement of a larger cohort and further analysis to validate the observations presented here, as well as testing the flexibility and complexity metrics in a control study against ageing and impaired subjects.

TABLE I
NUMBER OF VIBRATORY STIMULI (k) ACROSS SUBJECTS DURING THE 10 MIN TASK TRIAL IN BOTH EXPERIMENTAL CONDITIONS AND NUMBER OF 1 s EPOCHS FOLLOWING THE ONSET OF EACH VIBRATION THAT WERE ACCEPTED IN THE PREPROCESSING PHASE BECAUSE FREE FROM SIGNAL CORRUPTION

(A) OPEN EYES

Subj n.	Stimuli k	Accepted epochs
1	89	89
2	91	91
3	89	82
4	85	85
5	91	91
6	89	89
7	85	84
8	91	90
9	68	68
10	79	64
11	85	85

(B) CLOSED EYES

Subj n.	Stimuli k	Accepted epochs
1	89	87
2	85	61
3	85	38
4	87	64
5	89	89
6	91	54
7	89	89
8	89	57
9	85	85
10	89	54
11	87	56

VI. CONCLUSION

The goal of this work was to use the tools provided by network neuroscience to identify and shed light on the interplay between cortical regions that are predominantly involved in the high-level coordination of the postural control system, following a mechanical challenge to the participant's upright stance. Indeed, network neuroscience provides a valuable set of analysis tools that can complement the body of postural control literature, providing further insight into the mechanisms that govern brain functions.

The results show differences in the properties of cortical networks, both in individual regions and in the overall connectome structure during the postural task execution, between the experimental conditions of open and closed eyes. While differences in individual nodes strength are backed by statistical significance, differences in the network connections only provide a qualitative support to the results and require further investigation on a larger cohort. Overall, the results highlight the proprioceptive, vestibular and visual pathways of cortical response that we would expect as a result of the mechanical skeletal muscle perturbation that was applied. In particular, they revealed the different cortical strategies put in place during open and closed eyes task, with a reliance on visual frontal pathways in the former case and vestibular and proprioceptive temporal-parietal pathways in the latter. Moreover, the assessment of the flexibility of cortical regions provides valuable insights on the subject's ability to dynamically reconfigure the modular structure of their cortical

TABLE II
NODEWISE STATIC ANALYSIS RESULTS. LIST OF CORTICAL REGIONS WHICH SHOWED A SIGNIFICANT STRENGTH INCREASE IN OPEN EYES (A) AND CLOSED EYES (B), COMPARED TO THE OPPOSITE CONDITION. ALSO REPORTED ARE THE AVERAGE STRENGTH VALUE ACROSS SUBJECTS AND ASSOCIATED STANDARD DEVIATION, AS WELL AS THE PERCENTAGE INCREASE OVER THE OPPOSITE CONDITION AND RELATIVE p-VALUE

(A) OPEN EYES

	Region Name	Strength value	SD	Strength Increase (%)	p-val
Left	l.parsorbitalis	3.5	1.6	62.3	0.024
	l.caudalanteriorcingulate	4.1	1.5	47.5	0.033
	l.medialorbitofrontal	5.1	2.4	38.3	0.033
	l.lateralorbitofrontal	3.0	1.4	56.9	0.036
	l.superiorfrontal	6.6	2.3	28.9	0.036
	l.isthmuscingulate	7.2	4.2	15.9	0.039
	l.caudalmiddlefrontal	4.7	2.5	55.8	0.044
Right	r.caudalmiddlefrontal	8.9	2.2	26.9	0.015
	r.lateralorbitofrontal	5.4	1.8	58.6	0.015
	r.medialorbitofrontal	5.5	2.1	56.3	0.015
	r.parsopercularis	8.8	1.8	26.5	0.015
	r.rostralanteriorcingulate	6.5	2.3	48.2	0.015
	r.superiorfrontal	7.3	2.5	45.4	0.015
	r.temporalpole	7.2	2.7	39.1	0.015
	r.parstriangularis	7.3	1.9	37.8	0.044

(B) CLOSED EYES

	Region Name	Strength value	SD	Strength Increase (%)	p-val
Left	l.supramarginal	24.9	3.0	22.5	0.033
	l.parahippocampal	26.1	3.5	21.2	0.036
	l.precuneus	25.6	3.7	16.1	0.036
Right	r.bankssts	25.5	3.9	16.6	0.015
	r.fusiform	27.3	3.4	22.4	0.015
	r.inferiortemporal	25.9	3.3	20.5	0.015
	r.isthmuscingulate	20.1	4.8	3.9	0.015
	r.lingual	25.9	4.5	25.5	0.015
	r.superiorparietal	25.1	4.6	19.1	0.015
	r.postcentral	23.5	4.2	20.2	0.031
	r.inferiorparietal	21.2	4.5	16.6	0.033
	r.supramarginal	24.8	3.4	25.1	0.033
	r.paracentral	25.5	3.7	22.1	0.036
	r.superiortemporal	21.9	4.0	24.2	0.036

TABLE III
EDGEWISE STATIC ANALYSIS RESULTS. LIST OF CORTICAL REGIONS THAT ARE PART OF THE NETWORK AND CORRESPONDING DEGREE

	(A) TASK		(B) BASELINE	
	Region Name	Deg	Region Name	Deg
Left	l.precuneus	14	l.bankssts	17
	l.bankssts	13	l.fusiform	17
	l.fusiform	12	l.medialorbitofrontal	14
	l.inferiortemporal	11	l.inferiortemporal	13
	l.supramarginal	8	l.parsopercularis	11
	l.parahippocampal	5	l.precuneus	11
	l.inferiorparietal	4	l.superiortemporal	10
	l.lateralorbitofrontal	3	l.supramarginal	10
	l.precentral	3	l.parahippocampal	9
	l.rostralanteriorcingulate	2	l.pericalcarine	9
	l.rostralmiddlefrontal	2	l.insula	8
	l.middletemporal	1	l.posteriorcingulate	8
	l.pericalcarine	1	l.superiorfrontal	8
			l.middletemporal	7
			l.transversetemporal	6
			l.cuneus	3
			l.entorhinal	3
			l.paracentral	3
			l.postcentral	3
			l.parsorbitalis	2
Right	r.lingual	15	r.lingual	24
	r.superiorparietal	14	r.superiorparietal	15
	r.inferiorparietal	13	r.transversetemporal	12
	r.postcentral	13	r.postcentral	11
	r.transversetemporal	13	r.fusiform	9
	r.fusiform	12	r.inferiortemporal	8
	r.inferiortemporal	12	r.middletemporal	8
	r.middletemporal	10	r.superiortemporal	8
	r.supramarginal	10	r.bankssts	7
	r.bankssts	9	r.parsorbitalis	6
	r.isthmuscingulate	7	r.posteriorcingulate	6
	r.paracentral	7	r.precuneus	5
	r.precuneus	6	r.rostralmiddlefrontal	5
	r.posteriorcingulate	4	r.paracentral	4
	r.parahippocampal	3	r.precentral	4
	r.superiortemporal	3	r.entorhinal	3
	r.cuneus	1	r.supramarginal	3
	r.rostralanteriorcingulate	1	r.parahippocampal	2
			r.caudalanteriorcingulate	1
			r.insula	1
			r.medialorbitofrontal	1
			r.parstriangularis	1
			r.rostralanteriorcingulate	1

TABLE IV
FLEXIBILITY/ COMPLEXITY CORRELATION RESULTS. LIST OF CORTICAL REGIONS ASSOCIATED WITH A SIGNIFICANT PEARSON'S CORRELATION COEFFICIENT

	Region Name	Pearson's ρ	p-val
Right	r.supramarginal	0.66	0.026
	r.posteriorcingulate	0.69	0.019
	r.postcentral	0.65	0.032
	r.middletemporal	0.81	0.002
	r.isthmuscingulate	0.80	0.003
	r.inferiorparietal	0.63	0.039
	r.cuneus	0.70	0.018
	r.bankssts	0.72	0.012

network over time, in response to external stimuli or tasks. At the same time, complexity of the posturographic signal has been recognized as a hallmark of a healthy postural control system's ability to respond and adapt to external perturbations and cognitive stressors, reflecting the presence of a "highly adaptable network of neuro-muscular connections" [62], [78].

Overall, the fact that high flexibility emerges in the reported regions of the temporal, parietal and cingulate cortex is coherent with their involvement in highly integrative functions characterized by complex interconnections of visual, proprioceptive and vestibular processes. It is interesting to observe how clearly the flexibility index of these regions correlates with a well-established index of postural performance, easily obtainable through posturographic analysis of the body sway. This suggests the possibility of employing the flexibility of those network nodes as a marker to denote a healthy and effective postural control system. Furthermore, in addition to being a neurological diagnostic tool to detect early signs of postural functions decline, it could be of interest in the development of neurofeedback strategies aimed at improving postural performances by enhancing the flexibility of those cortical areas via targeted cognitive training or local stimulation techniques.

TABLE V

S_{EN} VALUES (MEAN ± SD) DURING BASELINE AND TASK, IN THE TWO EXPERIMENTAL CONDITIONS OE AND CE, FOR AP AND ML SWAY (TABLE A AND B RESPECTIVELY). THE LAST COLUMN OF EACH TABLE REPORTS THE p-VALUES RESULTING FROM A WILCOXON SIGNED-RANK TEST PERFORMED IN BASELINE AND TASK BETWEEN CONDITIONS (OE VS. CE). THE LAST ROW REPORTS THE p-VALUES RESULTING FROM A WILCOXON SIGNED-RANK TEST PERFORMED BETWEEN BASELINE AND TASK, FOR BOTH CONDITIONS. ASTERISKS HIGHLIGHT SIGNIFICANT p-VALUES ($p < 0.05$)

(A) AP

	OE	CE	p-val (OE vs. CE)
BASE	0.0176 ± 0.0057	0.0169 ± 0.0070	0.7
TASK	0.0246 ± 0.0062	0.0219 ± 0.0051	* 0.042
p-val (BASE vs. TASK)	* 0.001	* 0.002	

(B) ML

	OE	CE	p-val (OE vs. CE)
BASE	0.0286 ± 0.0279	0.0268 ± 0.0382	0.4131
TASK	0.0373 ± 0.0435	0.0262 ± 0.0245	* 0.0029
p-val (BASE vs. TASK)	0.0537	0.0537	

APPENDIX

See Tables I–V.

REFERENCES

[1] A. Fornito, A. Zalesky, and E. T. Bullmore, *Fundamentals of Brain Network Analysis*. Amsterdam, The Netherlands: Elsevier, 2016.

[2] D. Johnston and S. M.-S. Wu, *Foundations of Cellular Neurophysiology*. Cambridge, MA, USA: MIT Press, 1995.

[3] T. Mergner, C. Maurer, and R. J. Peterka, "A multisensory posture control model of human upright stance," *Prog. Brain Res.*, vol. 142, pp. 189–201, Jan. 2003.

[4] E. V. Sullivan, J. Rose, T. Rohlfing, and A. Pfefferbaum, "Postural sway reduction in aging men and women: Relation to brain structure, cognitive status, and stabilizing factors," *Neurobiol. Aging*, vol. 30, no. 5, pp. 793–807, May 2009.

[5] C.-C. Lin, J. W. Barker, P. J. Sparto, J. M. Furman, and T. J. Huppert, "Functional near-infrared spectroscopy (fNIRS) brain imaging of multisensory integration during computerized dynamic posturography in middle-aged and older adults," *Exp. Brain Res.*, vol. 235, no. 4, pp. 1247–1256, Apr. 2017.

[6] R. A. Ozdemir, J. L. Contreras-Vidal, B.-C. Lee, and W. H. Paloski, "Cortical activity modulations underlying age-related performance differences during posture–cognition dual tasking," *Exp. Brain Res.*, vol. 234, no. 11, pp. 3321–3334, Nov. 2016.

[7] B. T. T. Yeo *et al.*, "The organization of the human cerebral cortex estimated by intrinsic functional connectivity," *J. Neurophysiol.*, vol. 106, no. 3, pp. 1125–1165, Sep. 2011.

[8] M. M. Wierzbicka, J. C. Gilhodes, and J. P. Roll, "Vibration-induced postural posteffects," *J. Neurophysiol.*, vol. 79, no. 1, pp. 143–150, 1998.

[9] J. P. Roll, J. P. Vedel, and E. Ribot, "Alteration of proprioceptive messages induced by tendon vibration in man: A microneurographic study," *Exp. Brain Res.*, vol. 76, no. 1, pp. 213–222, Jun. 1989.

[10] P. A. Fransson, A. Hafström, M. Karlberg, M. Magnusson, A. Tjäder, and R. Johansson, "Postural control adaptation during galvanic vestibular and vibratory proprioceptive stimulation," *IEEE Trans. Biomed. Eng.*, vol. 50, no. 12, pp. 1310–1319, Dec. 2003.

[11] N. Toosizadeh, H. Ehsani, M. Miramonte, and J. Mohler, "Proprioceptive impairments in high fall risk older adults: The effect of mechanical calf vibration on postural balance," *Biomed. Eng. OnLine*, vol. 17, no. 1, pp. 1–14, May 2018.

[12] F. Barollo *et al.*, "Postural control adaptation and habituation during vibratory proprioceptive stimulation: An HD-EEG investigation of cortical recruitment and kinematics," *IEEE Trans. Neural Syst. Rehabil. Eng.*, vol. 28, no. 6, pp. 1381–1388, Jun. 2020.

[13] K. J. Edmunds *et al.*, "Cortical recruitment and functional dynamics in postural control adaptation and habituation during vibratory proprioceptive stimulation," *J. Neural Eng.*, vol. 16, no. 2, Apr. 2019, Art. no. 026037.

[14] J. Zhou, L. Lipsitz, D. Habtemariam, and B. Manor, "Sub-sensory vibratory noise augments the physiologic complexity of postural control in older adults," *J. NeuroEng. Rehabil.*, vol. 13, no. 1, p. 44, Dec. 2016.

[15] L. Cai, J. S. Y. Chan, J. H. Yan, and K. Peng, "Brain plasticity and motor practice in cognitive aging," *Frontiers Aging Neurosci.*, vol. 6, p. 31, Mar. 2014.

[16] M. Patel, P. A. Fransson, and M. Magnusson, "Effects of ageing on adaptation during vibratory stimulation of the calf and neck muscles," *Gerontology*, vol. 55, no. 1, pp. 82–91, 2009.

[17] D. Brunet, M. M. Murray, and C. M. Michel, "Spatiotemporal analysis of multichannel EEG: CARTOOL," *Comput. Intell. Neurosci.*, vol. 2011, pp. 1–15, Oct. 2011.

[18] L. C. Parra, C. D. Spence, A. D. Gerson, and P. Sajda, "Recipes for the linear analysis of EEG," *NeuroImage*, vol. 28, no. 2, pp. 326–341, Nov. 2005.

[19] J. Zhou, L. Lipsitz, D. Habtemariam, and B. Manor, "Sub-sensory vibratory noise augments the physiologic complexity of postural control in older adults," *J. NeuroEng. Rehabil.*, vol. 13, no. 1, pp. 1–8, Dec. 2016.

[20] S. F. Donker, M. Roerdink, A. J. Greven, and P. J. Beek, "Regularity of center-of-pressure trajectories depends on the amount of attention invested in postural control," *Exp. Brain Res.*, vol. 181, no. 1, pp. 1–11, Jul. 2007.

[21] A. Kabbara, V. Paban, and M. Hassan, "The dynamic modular fingerprints of the human brain at rest," *NeuroImage*, vol. 227, Feb. 2021, Art. no. 117674.

[22] M. Hassan and F. Wendling, "Electroencephalography source connectivity: Aiming for high resolution of brain networks in time and space," *IEEE Signal Process. Mag.*, vol. 35, no. 3, pp. 81–96, May 2018.

[23] H. Hallez *et al.*, "Review on solving the forward problem in EEG source analysis," *J. Neuroeng. Rehabil.*, vol. 4, no. 1, p. 46, Nov. 2007.

[24] S. Baillet, J. C. Mosher, and R. M. Leahy, "Electromagnetic brain mapping," *IEEE Signal Process. Mag.*, vol. 18, no. 6, pp. 14–30, Nov. 2001.

[25] F. Tadel, S. Baillet, J. C. Mosher, D. Pantazis, and R. M. Leahy, "Brainstorm: A user-friendly application for MEG/EEG analysis," *Comput. Intell. Neurosci.*, vol. 2011, Apr. 2011, Art. no. 879716.

[26] A. S. Hincapié *et al.*, "MEG connectivity and power detections with minimum norm estimates require different regularization parameters," *Comput. Intell. Neurosci.*, vol. 2016, Oct. 2016, Art. no. 3979547.

[27] R. Grech, T. Cassar, J. Muscat, K. P. Camilleri, S. G. Fabri, and M. Zervakis, "Review on solving the inverse problem in EEG source analysis," *J. Neuroeng. Rehabil.*, vol. 5, p. 25, Nov. 2008.

[28] R. S. Desikan *et al.*, "An automated labeling system for subdividing the human cerebral cortex on MRI scans into gyral based regions of interest," *NeuroImage*, vol. 31, no. 3, pp. 968–980, Jul. 2006.

[29] F. Wendling, P. Chauvel, A. Biraben, and F. Bartolomei, "From intracerebral EEG signals to brain connectivity: Identification of epileptogenic networks in partial epilepsy," *Frontiers Syst. Neurosci.*, vol. 4, p. 154, Nov. 2010.

[30] M. Hassan *et al.*, "Identification of interictal epileptic networks from dense-EEG," *Brain Topogr.*, vol. 30, no. 1, pp. 60–76, Jan. 2017.

[31] A. Kabbara, V. Paban, and M. Hassan, "The dynamic modular fingerprints of the human brain at rest," *Neuroimage*, vol. 227, Feb. 2021, Art. no. 117674.

[32] A. Zalesky, A. Fornito, and E. T. Bullmore, "Network-based statistic: Identifying differences in brain networks," *NeuroImage*, vol. 53, no. 4, pp. 1197–1207, Dec. 2010.

[33] V. D. Blondel, J.-L. Guillaume, R. Lambiotte, and E. Lefebvre, "Fast unfolding of communities in large networks," *J. Stat. Mech., Theory Exp.*, vol. 2008, no. 10, Oct. 2008, Art. no. P10008.

[34] D. S. Bassett and O. Sporns, "Network neuroscience," *Nature Neurosci.*, vol. 20, no. 3, pp. 353–364, Feb. 2017.

[35] C. S. Sherrington, "Flexion-reflex of the limb, crossed extension-reflex, and reflex stepping and standing," *J. Physiol.*, vol. 40, nos. 1–2, pp. 28–121, Apr. 1910.

[36] D. A. E. Bolton, "The role of the cerebral cortex in postural responses to externally induced perturbations," *Neurosci. Biobehav. Rev.*, vol. 57, pp. 142–155, Oct. 2015.

[37] A. Mierau, B. Pester, T. Hülsdünker, K. Schiecke, H. K. Strüder, and H. Witte, "Cortical correlates of human balance control," *Brain Topogr.*, vol. 30, no. 4, pp. 434–446, Jul. 2017.

[38] J.-M. Schoffelen and J. Gross, "Source connectivity analysis with MEG and EEG," *Hum. Brain Mapping*, vol. 30, no. 6, pp. 1857–1865, Jun. 2009.

[39] S. M. Peterson and D. P. Ferris, "Group-level cortical and muscular connectivity during perturbations to walking and standing balance," *NeuroImage*, vol. 198, pp. 93–103, Sep. 2019.

[40] J. A. Palmer, A. M. Payne, L. H. Ting, and M. R. Borich, "Cortical engagement metrics during reactive balance are associated with distinct aspects of balance behavior in older adults," *Front. Aging Neurosci.*, vol. 13, p. 410, Jul. 2021.

[41] H. Fujita, K. Kasubuchi, S. Wakata, M. Hiyamizu, and S. Morioka, "Role of the frontal cortex in standing postural sway tasks while dual-tasking: A functional near-infrared spectroscopy study examining working memory capacity," *BioMed Res. Int.*, vol. 2016, pp. 1–10, Oct. 2016.

[42] J. D. Schall, "Frontal eye fields," in *Encyclopedia of Neuroscience*. Berlin, Germany: Springer, 2008, pp. 1635–1638.

[43] S. Japee, K. Holiday, M. D. Satyshur, I. Mukai, and L. G. Ungerleider, "A role of right middle frontal gyrus in reorienting of attention: A case study," *Frontiers Syst. Neurosci.*, vol. 9, p. 23, Mar. 2015.

[44] R. Ptak, A. Schnider, and J. Fellrath, "The dorsal frontoparietal network: A core system for emulated action," *Trends Cogn. Sci.*, vol. 21, no. 8, pp. 589–599, Aug. 2017.

[45] M. L. Kringelbach, "The human orbitofrontal cortex: Linking reward to hedonic experience," *Nature Rev. Neurosci.*, vol. 6, no. 9, pp. 691–702, Sep. 2005.

[46] C. Lavin, C. Melis, E. Mikulan, C. Gelormini, D. Huepe, and A. Ibañez, "The anterior cingulate cortex: An integrative hub for human socially-driven interactions," *Frontiers Neurosci.*, vol. 7, p. 64, May 2013.

[47] S. Slobounov, C. Cao, N. Jaiswal, and K. M. Newell, "Neural basis of postural instability identified by VTC and EEG," *Exp. Brain Res.*, vol. 199, no. 1, pp. 1–16, Oct. 2009.

[48] M. A. Rapp, R. T. Krampe, and P. B. Baltes, "Adaptive task prioritization in aging: Selective resource allocation to postural control is preserved in Alzheimer disease," *Amer. J. Geriatric Psychiatry*, vol. 14, no. 1, pp. 52–61, Jan. 2006.

[49] M. Doumas, C. Smolders, and R. T. Krampe, "Task prioritization in aging: Effects of sensory information on concurrent posture and memory performance," *Exp. Brain Res.*, vol. 187, no. 2, pp. 275–281, May 2008.

[50] B. P. Delhaye, K. H. Long, and S. J. Bensmaia, "Neural basis of touch and proprioception in primate cortex," *Comprehensive Physiol.*, vol. 8, no. 4, pp. 1575–1602, Sep. 2018.

[51] H. O. Karnath, "Spatial orientation and the representation of space with parietal lobe lesions," *Philos. Trans. Roy. Soc. B, Biol. Sci.*, vol. 352, no. 1360, pp. 1411–1419, 1997.

[52] J. Ventre-Dominey, "Vestibular function in the temporal and parietal cortex: Distinct velocity and inertial processing pathways," *Frontiers Integrative Neurosci.*, vol. 8, p. 53, Jul. 2014.

[53] S. M. Frank and M. W. Greenlee, "The parieto-insular vestibular cortex in humans: More than a single area?" *J. Neurophysiol.*, vol. 120, no. 3, pp. 1438–1450, Sep. 2018.

[54] T. Brandt and M. Dieterich, "Does the vestibular system determine the lateralization of brain functions?" *J. Neurol.*, vol. 262, no. 1, pp. 214–215, Jan. 2015.

[55] P. Hlavackova and N. Vuillerme, "Do somatosensory conditions from the foot and ankle affect postural responses to plantar-flexor muscles fatigue during bipedal quiet stance?" *Gait Posture*, vol. 36, no. 1, pp. 16–19, May 2012.

[56] A. Kabbara *et al.*, "Detecting modular brain states in rest and task," *Netw. Neurosci.*, vol. 3, no. 3, pp. 878–901, Jan. 2019.

[57] C. L. Gallen *et al.*, "Modular brain network organization predicts response to cognitive training in older adults," *PLoS ONE*, vol. 11, no. 12, Dec. 2016, Art. no. e0169015.

[58] S. B. Chapman *et al.*, "Neural mechanisms of brain plasticity with complex cognitive training in healthy seniors," *Cerebral Cortex*, vol. 25, no. 2, pp. 396–405, Feb. 2015.

[59] D. S. Bassett, N. F. Wymbs, M. A. Porter, P. J. Mucha, J. M. Carlson, and S. T. Grafton, "Dynamic reconfiguration of human brain networks during learning," *Proc. Nat. Acad. Sci. USA*, vol. 108, no. 18, pp. 7641–7646, May 2011.

[60] P. G. Reddy *et al.*, "Brain state flexibility accompanies motor-skill acquisition," *NeuroImage*, vol. 171, pp. 135–147, May 2018.

[61] L. A. Lipsitz and A. L. Goldberger, "Loss of 'complexity' and aging: Potential applications of fractals and chaos theory to senescence," *J. Amer. Med. Assoc.*, vol. 267, no. 13, pp. 1806–1809, 1992.

[62] B. Manor and L. A. Lipsitz, "Physiologic complexity and aging: Implications for physical function and rehabilitation," *Prog. Neuro-Psychopharmacol. Biol. Psychiatry*, vol. 45, pp. 287–293, Aug. 2013.

[63] M. Costa, A. L. Goldberger, and C.-K. Peng, "Multiscale entropy analysis of complex physiologic time series," *Phys. Rev. Lett.*, vol. 89, no. 6, pp. 6–9, Jul. 2002.

[64] A. F. Ambrose, G. Paul, and J. M. Hausdorff, "Risk factors for falls among older adults: A review of the literature," *Maturitas*, vol. 75, no. 1, pp. 51–61, May 2013.

[65] S. W. Muir, K. Gopaul, and M. M. M. Odasso, "The role of cognitive impairment in fall risk among older adults: A systematic review and meta-analysis," *Age Ageing*, vol. 41, no. 3, pp. 299–308, May 2012.

[66] H. T. Karim *et al.*, "Functional MR imaging of a simulated balance task," *Brain Res.*, vol. 1555, pp. 20–27, Mar. 2014.

[67] A. Guterstam, M. Björnsdotter, G. Gentile, and H. H. Ehrsson, "Posterior cingulate cortex integrates the senses of self-location and body ownership," *Current Biol.*, vol. 25, no. 11, pp. 1416–1425, Jun. 2015.

[68] R. Leech, R. Braga, and D. J. Sharp, "Echoes of the brain within the posterior cingulate cortex," *J. Neurosci.*, vol. 32, no. 1, pp. 215–222, Jan. 2012.

[69] R. Leech and D. J. Sharp, "The role of the posterior cingulate cortex in cognition and disease," *Brain*, vol. 137, no. 1, pp. 12–32, Jan. 2014.

[70] S. Vanni, T. Tanskanen, M. Seppa, K. Uutelä, and R. Hari, "Coinciding early activation of the human primary visual cortex and anteromedial cuneus," *Proc. Nat. Acad. Sci. USA*, vol. 98, no. 5, pp. 2776–2780, Feb. 2001.

[71] H. Kolster, R. Peeters, and G. A. Orban, "The retinotopic organization of the human middle temporal area MT/V5 and its cortical neighbors," *J. Neurosci.*, vol. 30, no. 29, pp. 9801–9820, Jul. 2010.

[72] S. Gilaie-Dotan, A. P. Saygin, L. J. Lorenzi, R. Egan, G. Rees, and M. Behrmann, "The role of human ventral visual cortex in motion perception," *Brain*, vol. 136, no. 9, pp. 2784–2798, Sep. 2013.

[73] J. Billino, D. I. Braun, K.-D. Böhm, F. Bremmer, and K. R. Gegenfurtner, "Cortical networks for motion processing: Effects of focal brain lesions on perception of different motion types," *Neuropsychologia*, vol. 47, no. 10, pp. 2133–2144, Aug. 2009.

[74] L. M. Vaina, A. Cowey, R. T. Eskew, M. LeMay, and T. Kemper, "Regional cerebral correlates of global motion perception: Evidence from unilateral cerebral brain damage," *Brain*, vol. 124, no. 2, pp. 310–321, 2001.

[75] J. Xu *et al.*, "Tractography-based parcellation of the human middle temporal gyrus," *Sci. Rep.*, vol. 5, no. 1, pp. 1–13, Nov. 2016.

[76] K. Anton, A. Ernst, and D. Basta, "Auditory influence on postural control during stance tasks in different acoustic conditions," *J. Vestibular Res.*, vol. 29, no. 6, pp. 287–294, Jan. 2020.

[77] H. Petersen, M. Magnusson, R. Johansson, M. Akesson, and P. A. Fransson, "Acoustic cues and postural control," *Scand. J. Rehabil. Med.*, vol. 27, no. 2, pp. 99–104, 1995.

[78] M. A. Busa and R. E. A. van Emmerik, "Multiscale entropy: A tool for understanding the complexity of postural control," *J. Sport Health Sci.*, vol. 5, no. 1, pp. 44–51, Mar. 2016.